

1 **Revisiting and attributing the global controls on terrestrial**
2 **ecosystem functions of climate and plant traits at FLUXNET**
3 **sites via causal graphical models**

4 Haiyang Shi^{1,6}, Geping Luo^{2,3,4,6}, Olaf Hellwich⁷, Alishir Kurban^{2,3,4,6}, Philippe De Maeyer^{2,3,5,6} and Tim Van de
5 Voorde^{5,6}

6
7 ¹ School of Earth Sciences and Engineering, Hohai University, Nanjing 211100, China.

8 ² State Key Laboratory of Desert and Oasis Ecology, Xinjiang Institute of Ecology and Geography, Chinese
9 Academy of Sciences, Urumqi, Xinjiang, 830011, China.

10 ³ College of Resources and Environment, University of the Chinese Academy of Sciences, 19 (A) Yuquan Road,
11 Beijing, 100049, China.

12 ⁴ Research Centre for Ecology and Environment of Central Asia, Chinese Academy of Sciences, Urumqi, China.

13 ⁵ Department of Geography, Ghent University, Ghent 9000, Belgium.

14 ⁶ Sino-Belgian Joint Laboratory of Geo-Information, Ghent, Belgium.

15 ⁷ Department of Computer Vision & Remote Sensing, Technische Universität Berlin, 10587 Berlin, Germany.

16

17 **Correspondence to:** Geping Luo (luogp@ms.xjb.ac.cn) and Olaf Hellwich (olaf.hellwich@tu-berlin.de)

18 **Submitted to:** *Biogeosciences*

19

20 **Abstract**

21 Using statistical methods that not directly representing the causality between variables to attribute climate and
22 plant traits to control ecosystem function may produce biased perceptions. We revisit this issue using a causal
23 graphical model, Bayesian network (BN), capable of quantifying causality by conditional probability tables.
24 Based on expert knowledge and climate, vegetation, and ecosystem function data from the FLUXNET flux
25 stations, we constructed a BN containing the causal relationship of 'climate-plant trait-ecosystem function'.
26 Based on the sensitivity analysis function of the BN, we attributed the controls of climate and plant traits to
27 ecosystem function and compared the results with those based on Random forests and correlation analysis. The
28 main conclusions of this study include: BN can be used for the quantification of causal relationships between
29 complex ecosystems in response to climate change and enables the analysis of indirect effects among variables.
30 Compared to BN, the feature importance difference between 'mean vapor pressure deficit and cumulative soil
31 water index' and 'maximum leaf area index and maximum vegetation height' reported by Random forests is
32 higher and can be overestimated. With the causality relation between correlated variables constructed, BN-based
33 sensitivity analysis can reduce the uncertainty in quantifying the importance of correlated variables. The
34 understanding of the mechanism of indirect effects of climate variables on ecosystem function through plant
35 traits can be deepened by the chain causality quantification in BNs.

36 **1 Introduction**

37 Ecosystem function is the capacity of natural processes and components to provide goods and services that
38 satisfy human needs, either directly or indirectly (de Groot et al., 2002). Ecosystem functions include the
39 physicochemical and biological processes within the ecosystem to maintain terrestrial life. Terrestrial
40 ecosystems have provided a variety of important ecosystem functions for our society (Manning et al., 2018).
41 Plant traits' role as important determinants of ecosystem functions has been widely recognized (Chapin Iii et al.,
42 2000), and various trait syndromes can result in distinct broad differences in ecosystem functions (Reichstein et
43 al., 2014). In the context of global climate change, it is also essential to understand the potential changes in
44 ecosystem functions (Grimm et al., 2013). The response of terrestrial ecosystem function to changes in climate,
45 plant traits, and the corresponding mechanisms, are complex due to enormous spatial and temporal variations
46 across ecosystems, climate zones, and also space-time scales (Diaz and Cabido, 1997; Madani et al., 2018;
47 Myers-Smith et al., 2019). Given the enormous variations, on the global scale, these issues have not been
48 clarified well.

49
50 In the past decades, measurements of ecosystem functions are increasingly available to support studies of the
51 relations between ecosystem functions and climate variables. For example, eddy-covariance flux tower
52 observations (Baldocchi, 2014) for carbon flux (i.e., net ecosystem exchange (NEE)) and water flux (i.e.,
53 evapotranspiration (ET)) have been widely used to investigate changes in ecosystem functions and their
54 responses to climate change, vegetation condition changes, etc (Jung et al., 2020, 2010; Migliavacca et al., 2021;
55 Peaucelle et al., 2019). With the increase in such observations, various statistical analysis methods such as
56 emerging machine learning (Barnes et al., 2021; Migliavacca et al., 2021; Reichstein et al., 2019; Shi et al.,
57 2022b, a, 2020b; Tramontana et al., 2016) have been used to mine the hidden information on the effects of

58 climate change and its induced changes in vegetation, etc. on ecosystem function variables such as carbon and
59 water flux, which has not been understood in depth by process-based models (e.g., biogeochemistry models
60 (Sakschewski et al., 2016)). For example, using Random forests (RF) and principal component analysis (PCA),
61 a recent study (Migliavacca et al., 2021) quantified the three main axes of terrestrial ecosystem function and
62 their drivers based on observations of carbon and water fluxes of FLUXNET (Pastorello et al., 2020) and
63 various climate and plant trait variables. Generally, data-driven approaches have become increasingly important
64 recently in this area (Reichstein et al., 2019).

65

66 However, compared to the process-based models, most of these data-driven approaches lack representation of
67 the causality and detailed processes in the relations between ecosystem function and climate, despite the widely
68 recognized complex causal interactions of ecosystems with climate systems (Reichstein et al., 2014).

69 Conventional methods such as multiple linear regression have been questioned in attribution studies of the
70 relationship between climate and the carbon cycle (Wang et al., 2022). For example, the use of multiple linear
71 regression may underestimate the direct effect of soil moisture possibly due to the covariance between variables
72 (Wang et al., 2022). For machine learning techniques, current common algorithms such as RF (Migliavacca et
73 al., 2021) can report the importance of features (IMP) to measure their contributions to the prediction model.
74 However, IMP-based attribution to the target variable can also be unreliable if considerable confounders and
75 correlations between predictor variables exist (Strobl et al., 2008; Toloşi and Lengauer, 2011). The less relevant
76 predictors can replace the predictive predictors (due to correlation) and thus receive undeserved high feature
77 importance (Strobl et al., 2008). Correlations between predictors can lead to biased feature-importance-based
78 findings. It is thus important to recognize the difference between correlation and causality in these approaches,
79 represent detailed causal relations between features, rather than the unreliable feature importance rankings
80 generated from correlated features.

81

82 Bayesian network (BN) is a causal graphical model based on conditional probability representation (Friedman et
83 al., 1997; Pearl, 1985) that characterizes the transmission of cause and effect through conditional probabilities
84 between variables. Currently, BN has been used in modeling causal relationships in many fields and has
85 demonstrated advantages in causal interpretation, including in the fields such as hydrology and ecology (Chan et
86 al., 2010; Keshtkar et al., 2013; Milns et al., 2010; Pollino et al., 2007; Shi et al., 2021a, b; Trifonova et al.,
87 2015). However, BN has rarely been used in the study of the attribution of changes in ecosystem function.
88 Therefore, this study used BN to attribute the controls of climate and plant traits to ecosystem function by
89 quantifying the causal relationships involved. The data used are from a previous study (Migliavacca et al., 2021)
90 which extracted ecosystem function, climate, and plant trait variables for FLUXNET flux stations. The
91 construction of the causal structure of BN referred to the previous expert knowledge of this system (Reichstein
92 et al., 2014). Further, by comparing BN-based attribution analysis, linear correlation analysis, and RF-based
93 IMP reported by the previous study (Migliavacca et al., 2021), we investigated the adding-values of using BN
94 for causal analysis and discussed its prospects in this paper.

95 **2 Methodology**

96 **2.1 Data**

97 The used variables (Table 1) include the carbon and water fluxes of the FLUXNET flux tower sites and the
 98 ecosystem function variables derived from them, and information on the corresponding climate variables as well
 99 as plant traits:

- 100 a) Ecosystem function variables: underlying Water Use Efficiency (uWUE), maximum evapotranspiration
 101 (ETmax), maximum surface conductance (GSmax), maximum net CO₂ uptake of the ecosystem
 102 (NEPmax), Gross Primary Productivity at light saturation (GPPsat), Mean basal ecosystem respiration at a
 103 reference temperature of 15 °C (Rb), and apparent carbon-use efficiency (aCUE).
 104 b) Plant trait variables: ecosystem scale foliar nitrogen concentration (Nmass), Maximum Leaf Area Index
 105 (LAI_{max}), Maximum vegetation height (Hc). Of the total 202 sites (Migliavacca and Musavi, 2021), 101
 106 sites have Nmass data, 153 sites have LAI_{max} data, and 199 sites have Hc data. Only 98 have data on all
 107 these three plant trait variables.
 108 c) Climate variables: mean incoming shortwave radiation (SWin), Mean temperature (Tair), Mean Vapor
 109 Pressure Deficit (VPD), Mean annual precipitation (P), and cumulative soil water index (CSWI).

110

111 These data have different producing processes, including those calculated from flux data, site records, extracted
 112 from remote sensing data, etc. The detailed calculation methods can be found in the ref. (Migliavacca et al.,
 113 2021).

114

115 Table 1. The variables used and the discretization of their values in BN.

Variable node	Definition and units	Type	Approach (Migliavacca et al., 2021)	Discretization in BN (equal quantile thresholds: 0%, 33.33%, 66.67%, and 100% percentile values)
uWUE	underlying Water Use Efficiency [gC kPa ^{0.5} kgH ₂ O ⁻¹]	Ecosystem function	It was calculated from GPP, VPD, and ET (Zhou et al., 2014). The median of the half-hourly retained uWUE values was used for each site. It was further filtered by the following conditions: (i) SWin > 200 W m ⁻² ; (ii) no precipitation event for the last 24 hours, when precipitation data are available; and (iii) during the growing season: daily GPP > 30% of its seasonal amplitude.	0.068, 2.51, 3.18, 5.332
ETmax	maximum evapotranspiration in the growing season [mm]	Ecosystem function	ETmax was computed as the 95th percentile of ET in the growing season. It was also filtered by the same filtering applied to the uWUE calculation.	0.059, 0.17, 0.23, 0.423
GSmax	maximum surface conductance [m s ⁻¹]	Ecosystem function	GSmax was computed by inverting the Penman-Monteith equation after calculating the aerodynamic conductance. The 90th percentile of the half-hourly GS of each site was calculated and used as the GSmax of each site.	0.0013, 0.0077, 0.0123, 0.0566

NEPmax	maximum net CO ₂ uptake of the ecosystem [$\mu\text{mol CO}_2 \text{ m}^{-2} \text{ s}^{-1}$]	Ecosystem function	NEPmax was computed as the 90th percentile of the half-hourly net ecosystem production in the growing season (when daily GPP is > 30% of the GPP amplitude).	1.953, 15.3, 24.4, 42.82
GPPsat	Gross Primary Productivity at light saturation [$\mu\text{mol CO}_2 \text{ m}^{-2} \text{ s}^{-1}$]	Ecosystem function	GPPsat was computed as the 90th percentile estimated from half-hourly data by fitting the hyperbolic light response curves. The 90th percentile from the GPPsat estimates of each site was extracted.	3.042, 17.49, 27.74, 47.6
Rb	Mean basal ecosystem respiration at a reference temperature of 15 °C [$\mu\text{mol CO}_2 \text{ m}^{-2} \text{ s}^{-1}$]	Ecosystem function	Rb was derived from night-time NEE measurements. For each site, the mean of the daily Rb value was computed.	0.144, 2.07, 3.12, 10.67
aCUE	apparent carbon-use efficiency	Ecosystem function	aCUE was calculated by $\text{aCUE} = 1 - (\text{Rb}/\text{GPP})$ and the median value of daily aCUE is used.	-1.19, 0.4, 0.74, 1
Nmass	ecosystem scale foliar nitrogen concentration [$\text{gN } 100 \text{ g}^{-1}$]	Plant trait	Nmass was computed as the community-weighted average of foliar N% of the major species at the site sampled at the peak of the growing season or gathered from the literature (Musavi et al., 2016, 2015; Fleischer et al., 2015; Flechard et al., 2020).	0.65, 1.15, 1.76, 4.44
LAI _{max}	Maximum Leaf Area Index [$\text{m}^2 \text{ m}^{-2}$]	Plant trait	LAI _{max} was collected from the literature (Migliavacca et al., 2011; Flechard et al., 2020), the FLUXNET Biological Ancillary Data Management (BADM) product, and/or site principal investigators.	0.17, 2.27, 4.5, 12.9
Hc	Maximum vegetation height [m]	Plant trait	Hc was collected from the literature (Migliavacca et al., 2011; Flechard et al., 2020), the BADM product, and/or site principal investigators.	0.04, 1.7, 16.0, 80.1
SW _{in}	Mean incoming shortwave radiation [W m^{-2}]	Climate	SW _{in} was from FLUXNET data.	54.43, 134.18, 182.44, 266.04
T _{air}	Mean temperature [degree C]	Climate	T _{air} was from FLUXNET data.	-10.45, 6.62, 14.73, 28.1
VPD	Mean Vapor Pressure Deficit [hPa]	Climate	VPD was from FLUXNET data.	0.62, 3.38, 5.76, 26.08
P	Mean annual precipitation [cm/year]	Climate	P was from FLUXNET data.	5.51, 45.28, 79.29, 256.61

CSWI	cumulative soil water index	Climate-related soil water availability	CSWI was computed as a measure of water availability (Nelson et al., 2018).	-93.49, -1.24, 2.01, 4.47
------	-----------------------------	---	---	---------------------------

116

117 **2.2 BN for analyzing causal relations**

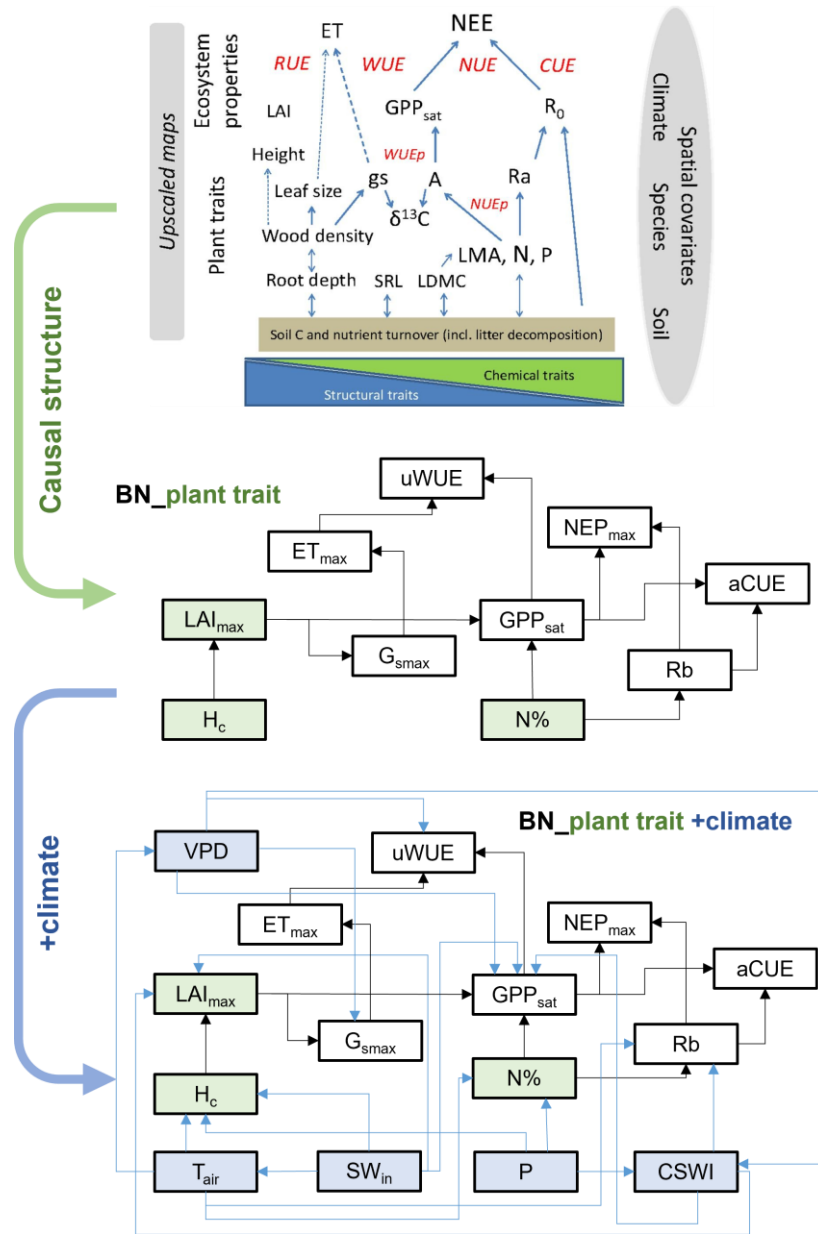
118 **2.2.1 BN structures**

119 Based on expert knowledge (Reichstein et al., 2014), we constructed the structure of BN containing the causal
 120 relationships between plant traits and ecosystem function variables: 'BN_plant_trait'. The causal links between
 121 the variables were referred to the relationship diagram in the upper part of Figure 1. Further, we added the
 122 climate variables and the corresponding causal relationships, expanding 'BN_plant_trait' to
 123 'BN_plant_trait_climate', which further incorporates the climate variables and their impacts on the system
 124 (Figure 1).

125

126 Each node is discretized for the BN compiling by the software Netica. The equal quantile (Nojavan A. et al.,
 127 2017) three-level discretization (the distribution of nodes (Figure S1) is divided into three levels) for each node
 128 is applied by the discretization thresholds of 0%, 33.33%, 66.67%, and 100% percentile values of the data
 129 distribution (Table 1) given the limitation of the amount of training data.

Expert Knowledge - Reichstein et al., 2014



130
131
132
133
134
135
136
137
138

Figure 1. The structure of two Bayesian networks (BNs) for attribution of variations in ecosystem functions. 'BN_plant_trait' in the median part incorporated the causal effects of plant traits (box in slight green) on ecosystem functions (box in white) from expert knowledge as the relation diagram on the upper part (Reichstein et al., 2014). 'BN_plant_trait_climate' in the lower part further incorporated the causal impacts of climate variables (box in light blue).

Table 2. Explanation of the added causal links between climate variable nodes, plant trait nodes, and ecosystem function variable nodes in the BNs.

Casual links		Explanation	References
Parent node	Child node		

VPD	uWUE	$uWUE = GPP \cdot VPD^{0.5} / ET$	(Zhou et al., 2014)
VPD	GSmax	stomatal and surface conductance declines under an increase in VPD	(Grossiord et al., 2020; Wever et al., 2002)
VPD	GPPsat	leaf and canopy photosynthetic rates decline when atmospheric VPD increases due to stomatal closure	(Yuan et al., 2019; Konings et al., 2017)
Tair	VPD	higher air temperature corresponds to higher saturated water vapor pressure and can drive an increase in VPD	(Yuan et al., 2019)
Tair	Hc	the temperature limitation on canopy height variation	(Moles et al., 2009)
Tair	Nmass	increase in air temperature may decrease plant nitrogen concentration and leaf nitrogen content.	(Weih and Karlsson, 2001; Reich and Oleksyn, 2004)
Tair	Rb	temperature strongly influences Rb through the laws of thermodynamics	(Davidson and Janssens, 2006; Enquist et al., 2003; Brown et al., 2004)
SWin	LAI _{max}	solar radiation affects vegetation conditions and phenology	(Günter et al., 2008; Liu et al., 2016; Borchert et al., 2015; Wagner et al., 2017)
SWin	Hc	solar radiation affects the distribution and composition of ecosystems through photosynthesis and the water cycle	(Borchert et al., 2015; Guisan and Zimmermann, 2000; Piedallu and Gégout, 2007)
SWin	GPPsat	solar radiation affects ecosystem productivity and plant growth	(Monteith, 1972; Borchert et al., 2015; Guisan and Zimmermann, 2000)
P	Hc	the hydraulic limitation hypothesis on canopy height variation	(Moles et al., 2009; Ryan and Yoder, 1997; Koch et al., 2004)
P	Nmass	leaf nitrogen concentration per unit mass may decrease with increasing precipitation	(Santiago and Mulkey, 2005; Wright and Westoby, 2002)
CSWI	LAI _{max}	soil moisture affects vegetation conditions	(Patanè, 2011)
CSWI	Rb	soil moisture affects the temperature dependence of ecosystem respiration	(Xu et al., 2004; Flanagan and Johnson, 2005; Wen et al., 2006)
CSWI	GPPsat	soil moisture can reduce GPP through ecosystem water stress	(Green et al., 2019)

139

140 2.2.2 BN evaluation and node sensitivity analysis

141 Based on the Bayesian network (BN), the joint impacts of multiple variables and their causal relations are
142 analyzed. A BN can be represented by nodes X_1, X_2, X_3 to X_n and the joint distribution (Pearl, 1985):

143
$$Pa(X) = Pa(X_1, X_2, \dots, X_n) = \prod_{i=1}^n Pa(X_i | pa(X_i)) \quad (1)$$

144 where $pa(X_i)$ is the probability of the parent node X_i . Expectation-maximization (Moon, 1996) is used to address
 145 the data with missing values and then compile the BN.

146
 147 We used k-fold cross-validation to verify the reliability of the BN. The k-fold approach has been widely used in
 148 previous studies for the validation of BNs (Marcot, 2012). In this study, k is set as 10 as commonly used
 149 (Marcot and Hanea, 2021). We choose ETmax, GPPsat, and NEPmax for cross-validation of accuracy, and the
 150 predicted status (status with the highest probability bar value) of the nodes will be compared with the actual
 151 status and the classification accuracy will be calculated.

152
 153 Sensitivity analysis is used for the evaluation of the strength of the causal relations between nodes based on
 154 mutual information (MI). MI is calculated as the entropy reduction of the child node resulting from changes
 155 found at the parent node (Shi et al., 2020a):

156
$$MI = H(Q) - H(Q|F) = \sum_q \sum_f P(q, f) \log_2 \left(\frac{P(q, f)}{P(q)P(f)} \right) \quad (2)$$

157 where H represents the entropy, Q represents the target node, F represents the set of other nodes and q and f
 158 represent the status of Q and F. In this study, we assessed the sensitivity of ecosystem function variables to
 159 climate and plant trait variables.

160 **2.2.3 Comparing different approaches used for attribution analysis**

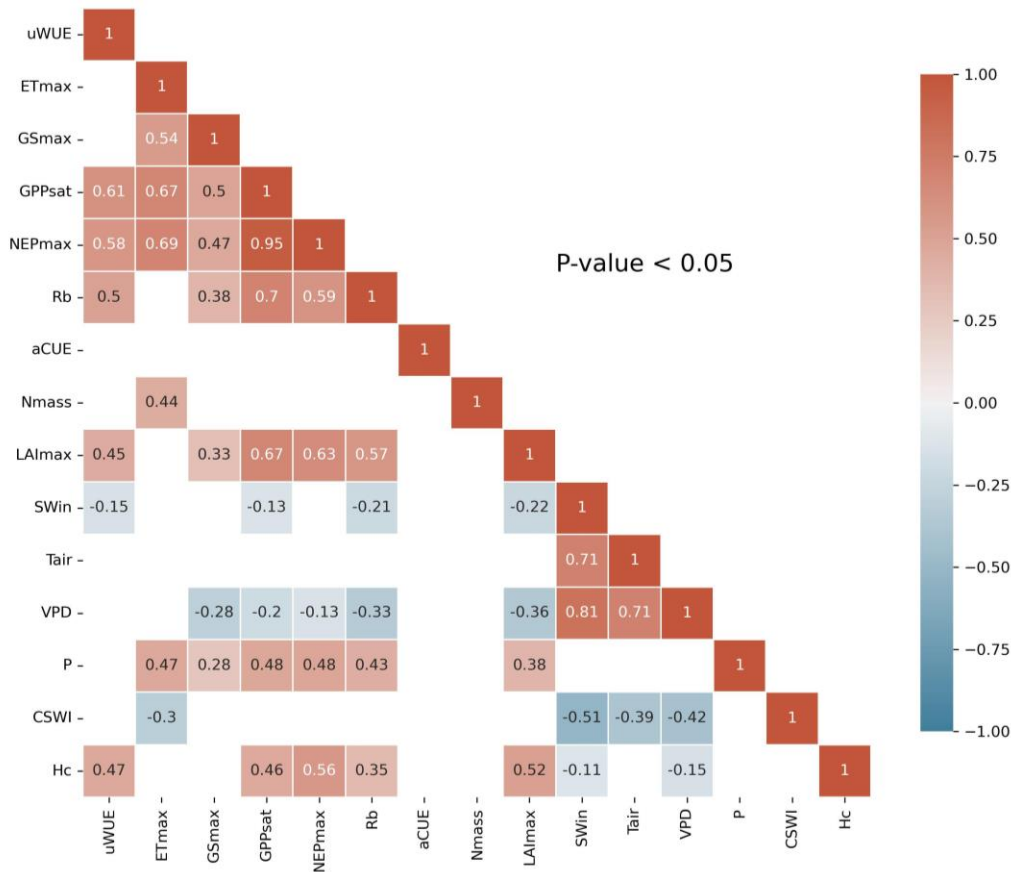
161 Further, to clarify the adding-values of considering causality in the attribution analysis of controls on ecosystem
 162 functions, the results of the BN-based sensitivity analysis (BN_sens) were compared with the other two
 163 approaches. They are the results of the absolute values of additional linear correlation analysis (linear_corr) in
 164 this study and the findings from the ref. (Migliavacca et al., 2021) using RF feature importance (RF_imp).
 165 BN_sens and linear_corr directly measure the effects of plant traits and climate variables on ecosystem function
 166 variables, while RF_imp measures their effects on the three principal components (PC1, PC2, and PC3) of
 167 ecosystem function variables, which were reported as the three major axes of ecosystem function by the ref.
 168 (Migliavacca et al., 2021). It was obtained from principal component analysis of 12 ecosystem function
 169 variables which included the six variables uWUE, ETmax, GSmax, NEPmax, GPPsat, and Rb used in the
 170 methods BN_sens and linear_corr. The first axis (PC1) explains 39.3% of the variance and is dominated by
 171 maximum ecosystem productivity properties, as indicated by the loadings of GPPsat and NEPmax, and
 172 maximum evapotranspiration (ETmax). The second axis (PC2) explains 21.4% of the variance and refers to
 173 water-use strategies as shown by the loadings of water-use efficiency metrics, evaporative fraction, and GSmax.
 174 The third axis (PC3) explains 11.1% of the variance and includes key attributes that reflect the carbon-use
 175 efficiency of ecosystems. PC3 is dominated by apparent carbon-use efficiency, basal ecosystem respiration (Rb),
 176 and the amplitude of evaporative fraction (Migliavacca et al., 2021).

177

178 **3 Results**

179 **3.1 Correlation analysis**

180 Linear correlation analysis of the variables (Figure 2) showed significant ($P < 0.05$) linear correlations between
 181 the ecosystem function variables and some of the climate and plant trait variables. SWin and VPD showed
 182 negative correlations with these ecosystem function variables. LAImax/ Hc showed significant positive
 183 relationships with most of the ecosystem function variables and significant negative relationships with SWin and
 184 VPD. Nmass only showed a positive relationship with ETmax. In addition, the majority of the ecosystem
 185 function variables showed significant ($P < 0.05$) positive correlations with each other.



186
 187 Figure 2. Correlation coefficient matrix of ecosystem functions and climate and plant trait variables for
 188 FLUXNET sites. Only correlation coefficients with p-values less than 0.05 level of significance is shown.

189 **3.2 BN-based analysis**

190 We compiled two different BNs (i.e., BN_plant_trait and BN_plant_trait_climate) (Figure 3) and found that the
 191 probability distributions of the values of the common nodes (ecosystem function and plant trait variable nodes)
 192 differed a little (e.g., in the probability distribution of LAImax, Hc, and Nmass) between the two BNs.

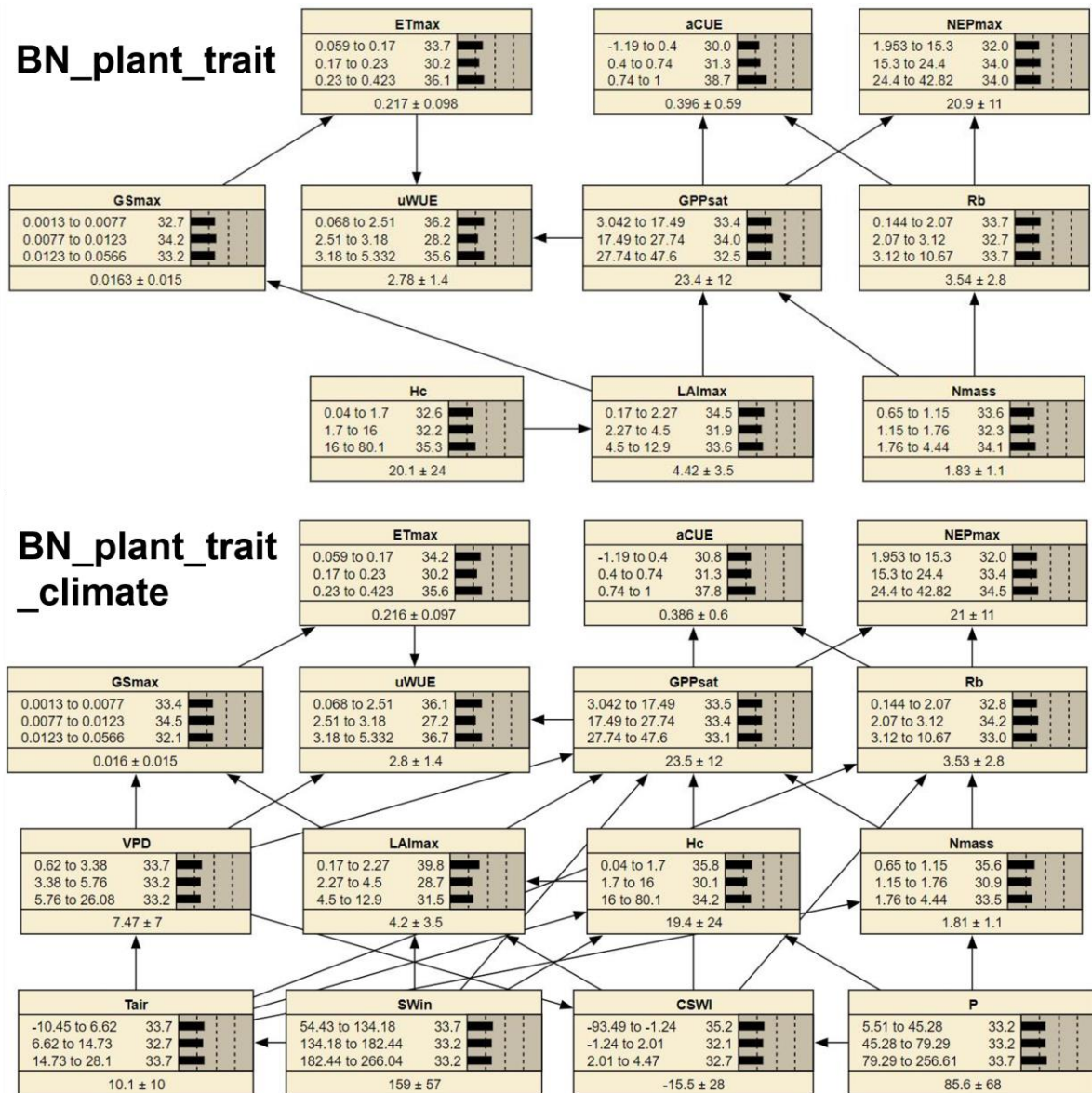
193 Compared to BN_plant_trait, in BN_plant_trait_climate, the climate variables of sites with missing plant trait
 194 data forced the changes in the probability distributions of LAImax, Hc, and Nmass. In the EM algorithm, for
 195 sites with missing plant trait data, existing relationships (obtained from observations from other sites) between
 196 plant trait variables and climate variables are used in the data interpolation of plant trait variables. In

197 BN_plant_trait, the added linkages of climate variables to plant trait variables resulted in higher
 198 probability values of the low-value status of the plant trait variables.

199

200 The 10-fold cross-validation of the nodes ETmax, GPPsat, and NEPmax showed relatively high accuracy. The
 201 classification accuracy (Table S1) of the status of ETmax was 60.9%, the classification accuracy of the status of
 202 NEPmax was 84.2% and the classification accuracy of the status of GPPsat was 75.2%.

203



204

205 Figure 3. The compiled two BNs ('BN_plant_trait' and 'BN_plant_trait_climate'). The bars of each node
 206 represent its probability distribution. At the bottom part of each node, the left and right side values of the '±'
 207 are the mean and standard deviation of the distribution, respectively.

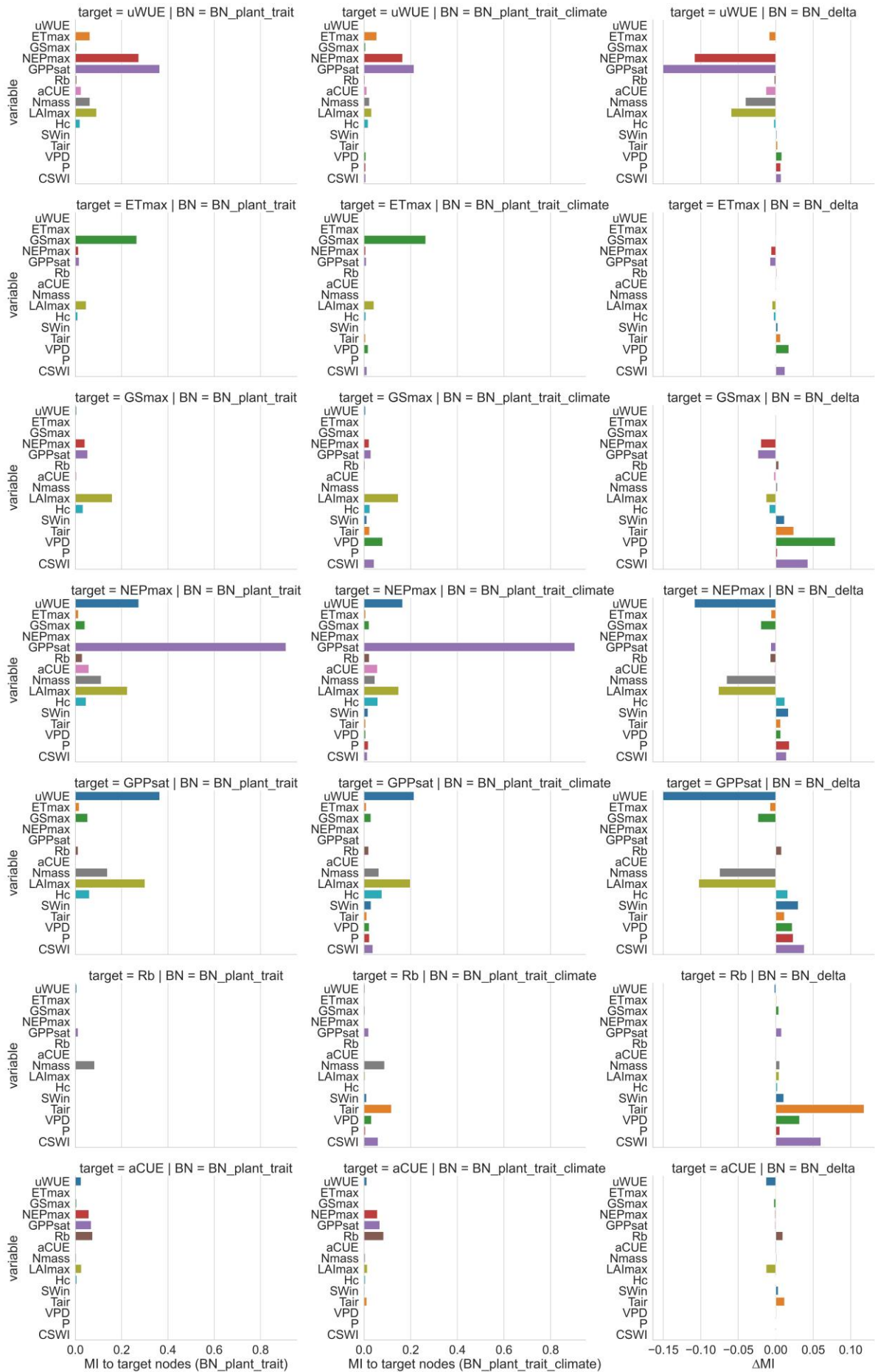
208

209 We performed sensitivity analyses (Figure 4) on the ecosystem function variables in both BNs to assess their
 210 sensitivity to various climate and plant trait variables. We also calculated the difference in sensitivity MI
 211 between the two BNs (Figure 4) to compare the change in sensitivity of ecosystem function to each variable

212 after adding further climate variables to the plant trait variables only. The sensitivity of different ecosystem
213 function variables to plant traits and climate variables was highly variable in both BNs. The magnitude of
214 sensitivity of ecosystem function nodes to plant traits and climate variables was related to whether these plant
215 traits and climate variables were set as their parent nodes. In BN_plant_trait, for the carbon fluxes GPPsat and
216 NEPmax, Nmass, and LAImax had higher sensitivity due to Nmass and LAI being set as their parent nodes. For
217 the water flux ETmax, it does not have high sensitivity to plant trait variables such as LAImax and Hc, although
218 these plant trait variables are set as the parent nodes of ETmax. This indicates the difference in the strength of
219 the control effects of plant traits on carbon and water fluxes.

220

221 In the sensitivity analysis of BN_plant_trait_climate, the sensitivity patterns of the ecosystem function variables
222 changed as a result of the inclusion of climate variables and the change in causality they introduced. The
223 sensitivity of the ecosystem function variables to climate variables was significantly increased (especially for
224 Tair, VPD, and CSWI). The control of plant traits on ecosystem function in BN_plant_trait is also partially
225 transformed into an indirect effect of climate variables by first controlling plant trait variables and then
226 controlling ecosystem function. For example, in BN_plant_trait_climate, for GPPsat, a decrease in the
227 sensitivity of GPPsat to LAImax and an increase in the sensitivity to Tair was observed after the causal chain of
228 Tair influencing Hc, LAImax, and then GPPsat was set. This can be explained by the fact that higher
229 temperatures promote vegetation growth and thus may increase LAImax, which then indirectly alters the
230 probability distribution of the GPPsat node. In previous studies based on statistical methods that did not consider
231 the chain causality, this indirect control on GPPsat from Tair may have been included in the contribution of
232 LAImax to GPPsat. Similarly, a chain causality of P by first affecting Nmass and then indirectly GPPsat was
233 also found. However, the effect of P by first affecting Hc, LAImax, and then indirectly affecting ETmax and
234 GSmax appears to be not large.



236 Figure 4. Sensitivity of ecosystem function variables to other variables in different networks based on mutual
237 information (MI). The left column is the sensitivity analysis of BN_plant_trait, the middle column is the
238 sensitivity analysis of BN_plant_trait_climate, and the right column is the difference between the reported
239 sensitivity of BN_plant_trait_climate and the sensitivity of BN_plant_trait. For BN_plant_trait, the MI values of
240 climate variables to ecosystem function variables are all 0 because they do not contain climate variables. For
241 each ecosystem function in these two BNs, its sensitivity to its child node is not shown (set as 0) because child
242 nodes are not considered causal variables and thus are not evaluated in the attribution.

243 **3.3 Comparing results from RF-based, BN-based analysis, and correlation analysis**

244 All three methods show the importance of the plant trait variables in explaining the variation of various
245 ecosystem function variables (Figure 5). LAImax was the most important of the three methods in explaining the
246 variation of maximum ecosystem productivity properties (corresponding to PC1). In contrast to the results of the
247 other two methods, in linear_corr, SWin and VPD were the least important, while P was more important.
248 Comparing RF_imp and BN_sens, the overall pattern of importance is similar, but there are differences. For
249 water-use strategies (corresponding to PC2), Hc is ranked first and LAI last in RF_imp, but in BN_sens, LAI is
250 slightly more important than Hc. In linear_corr, Hc and LAI are of similar importance. For PC3, VPD ranks first
251 and is more important than Tair in RF_imp. But in BN_sens, Tair is more important than VPD. Among the three
252 moisture-related climate variables (i.e., VPD, P, and CSWI), CSWI appears to be the least important in RF_imp
253 but is comparable to VPD in BN_sens.

254
255 Given the limitations of RF_imp in responding to the correlated variables (Strobl et al., 2008), the difference
256 between the significance of VPD and CSWI reported by RF_imp may be overestimated. For the ecosystem
257 functions related to water-use strategies, the difference between LAImax and Hc reported by BN_sens is also
258 much smaller than the difference reported by RF_imp. It implied that, with the causality relation between
259 correlated variables constructed, BN_sens reduced the uncertainty in quantifying the importance of correlated
260 variables.

	Methods	Nmass	LAI _{max}	Hc	SWin	Tair	VPD	P	CSWI
PC1	RF_imp	10.80%	16.60%	14.50%	7.60%	9.10%	11.70%	6.70%	4.00%
PC2	RF_imp	5.10%	4.50%	14.90%	10.70%	11.20%	7.40%	9.00%	8.30%
PC3	RF_imp	7.00%	2.80%	5.40%	9.30%	8.00%	15.40%	6.50%	4.90%
GPPsat	BN_sens	0.0635	0.1980	0.0766	0.0299	0.0116	0.0221	0.0232	0.0380
NEPmax	BN_sens	0.0464	0.1482	0.0588	0.0168	0.0064	0.0065	0.0181	0.0142
ETmax	BN_sens	0.0006	0.0424	0.0076	0.0028	0.0063	0.0174	0.0006	0.0122
uWUE	BN_sens	0.0228	0.0321	0.0174	0.0012	0.0023	0.0080	0.0066	0.0072
GSmax	BN_sens	0.0022	0.1464	0.0246	0.0115	0.0239	0.0793	0.0019	0.0429
Rb	BN_sens	0.0880	0.0043	0.0021	0.0106	0.1177	0.0317	0.0053	0.0602
aCUE	BN_sens	0.0049	0.0138	0.0056	0.0033	0.0117	0.0009	0.0004	0.0007
GPPsat	linear_corr		0.67	0.46	0.13		0.20	0.48	
NEPmax	linear_corr		0.63	0.56			0.13	0.48	
ETmax	linear_corr	0.44						0.47	0.30
uWUE	linear_corr		0.45	0.47	0.15				
GSmax	linear_corr						0.28		
Rb	linear_corr		0.57	0.35	0.21		0.33	0.43	
aCUE	linear_corr								

261
262 Figure 5. Comparisons of relationships of ecosystem functional variables to plant traits and climate variables in
263 different analyses. Method RF_imp is Random forest variable importance (Migliavacca et al., 2021) (see
264 Methodology section). Method linear_corr is Linear correlation analysis with the absolute values of Pearson
265 correlation coefficients (see Methodology section). Method BN_sens is a BN-based sensitivity analysis with
266 sensitivity values MI reported. The values in each method group are in red for high values and in blue for low
267 values.

268 4 Discussions

269 Based on BN, this study investigates the prospect of using causal graphical models to revisit and attribute the
270 control of climate and plant trait variations to ecosystem functions. Because of the inclusion of the constraints
271 provided by expert knowledge (Reichstein et al., 2014) and other perceptions from many previous studies, BN-
272 based attribution analysis is relatively reliable and can update our knowledge of the contribution of some
273 teleconnection variables through causal chains. The effective implementation of BN-based causal analysis may
274 depend on the reliability of the causal relationships provided by expert knowledge (directional links between
275 variables). We can establish the connection relationships and network structures between variables from expert
276 knowledge and assign the specific quantification of the connection relationships (conditional probability tables)

277 to observations (Shi et al., 2021a). If further combined with findings from process-based models, it is promising
278 to significantly improve our understanding of the complex ‘climate-plant trait-ecosystem function’ relationships
279 by comparing detailed relationships and structural influences between variables.

280

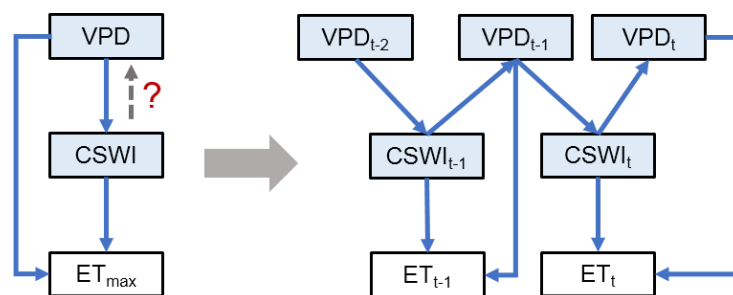
281 BN essentially factorizes the joint probability distribution among data variables into a series of conditional
282 probability distributions (Ramazi et al., 2021), and the reliability of this approach relies on the setting of causal
283 control relationships among nodes. Expert knowledge is thus critical in the construction of BNs, especially when
284 modeling complex systems. In addition to the causal relationship between nodes, the meaning represented by
285 each node, the data source/ approach, and the spatial and temporal resolution may also have impacts on the
286 results. For example, in this study, for multiple water use efficiency-related variables in the ref. (Migliavacca et
287 al., 2021), we chose uWUE, and for Rb, we chose the mean value of Rb. The results of BN-based analysis
288 may vary if different representations or meanings of nodes are selected. The way the data of each variable is
289 observed/ produced, the spatial and temporal resolution of the data, etc. can also affect the understanding of the
290 role of these variables in the data-driven BN. Some variables may be very important in the attribution of actual
291 ecosystem function variation, but their importance may be underestimated due to limitations in the inherent
292 observational accuracy of their data, and differences in their spatial and temporal scales from other variables. In
293 addition, some variables such as soil moisture may be difficult to obtain due to the lack of continuous site-scale
294 long-term observations. Using the water balance method to calculate CSWI as a proxy may introduce errors.
295 Since the CSWI calculation method relies on P, etc., the obtained relationship between P, CSWI, and other nodes
296 may have contained empirical components. If the availability of measurements of some nodes is low, modelers
297 should be cautious about the empirical dependencies with other nodes that may be included in the alternative
298 data approaches. Thus, the alternative use of multiple derivatives of a variable and data generated by different
299 methods for the construction of different BNs can help us to recognize how the uncertainty in the nodes and data
300 can influence BN-based attribution findings. Different node discretization schemes may also affect the
301 conditional probability table between nodes as well as the sensitivity (Nojavan A. et al., 2017). Other alternative
302 discretization schemes with the commonly used three levels may also be effective, such as using ‘mean-std’
303 (mean minus 1 standard deviation) and ‘mean+std’ (mean plus 1 standard deviation) as discretization thresholds,
304 which will result in a change in the relationship between BN nodes. And further if extreme values such as 5th
305 and 95th percentile are used in the node value discretization, it may be beneficial on quantifying the causal
306 control of extreme conditions of nodes on other nodes.

307

308 When considering higher-order effects (Bairey et al., 2016), the relationships between plant traits, climate
309 variables, and ecosystem function variables can be very complex. One variable may affect the relationship
310 between two other variables rather than directly affecting these two variables (Bairey et al., 2016). BN may have
311 limitations in directly analyzing such higher-order effects because BN requires the modeler to explicitly set
312 direct causal relationships between nodes. To analyze the higher-order effects, we can add nodes that directly
313 represent the relationship between the variables. For example, the correlation coefficient of two variables can be
314 used as a node and this node is connected to other nodes in the BN so that the control effect of other nodes on
315 this correlation coefficient can be explored. Such implements may be useful to deepen the impact of various
316 higher order effects.

317
318
319
320
321
322
323
324
325
326
327
328
329
330
331
332
333
334
335
336
337
338
339
340

Besides, the BN in this study was mainly based on data averaged over multiple years, thus possibly partially underestimating the effect of temporal variations in the relationships between variables. Another limitation of the BN proposed above is that the causal relationships between variables are unidirectional, while it is difficult to represent interactions and feedback between variables (Marcot and Penman, 2019). In future studies, to address these two issues, BN based on temporal dynamics can be promising (Figure 6). By refining the interaction of temporal lags between variables, it is possible to incorporate not only temporal variation but also control factors that attribute interactions and feedback between variables. For example, the interaction and feedback mechanisms of VPD, soil moisture, and ET with lag effects (Figure 6) and their impacts on ecosystems have attracted extensive interest from researchers (Anderegg et al., 2019; Humphrey et al., 2021; Lansu et al., 2020; Liu et al., 2020; Xu et al., 2022; Zhou et al., 2019), but conventional statistical methods have been ineffective in analyzing such relationships with both interactive causality and temporal lags. In contrast, the BN proposed here, which incorporates feedback effects and lagged effects that were common in climate-ecosystem relations (Lin et al., 2019), is potentially able to address this issue from a data-driven approach. In the practical modeling, different periods of the same node may still be not independent. Therefore, the split scheme of such periods may be critical. For example, a period between two precipitation events can be treated as one sample, which can enhance independence between periods. Subsequently, a such period can be divided into smaller periods such as t , $t-1$, $t-2$, etc. to aggregate the node values to appropriate time scales. Thus one sample can represent the interaction relationship between variables with lags in this period. Finally, we can integrate records of such periods between two precipitation events from sites across different climate zones and biomes to build synthesis models for global analysis of such problems. If further combined with the findings of process-based models, our understanding of climate and ecosystem interactions and feedback and their mechanisms in time is hopefully deepened.



341
342
343
344
345
346
347

Figure 6. The future BNs with the temporal causality further considered addressing the causality of the interaction between variables. The VPD-CSWI-ET relationship is used here as an example. t , $t-1$, and $t-2$ denote the current period, the last period, and the period before the last period, respectively. The network on the left only considers the effect of VPD on CSWI without considering the feedback of CSWI on the VPD. The network on the right characterizes the VPD-CSWI interaction with the feedback from CSWI at period $t-1$ to VPD at period t .

348 **5 Conclusion**

349 Based on BN, we revisited and attributed the contribution of climate and plant traits to global terrestrial
350 ecosystem function. The major conclusions of this study include:

- 351 1. BN can be used for the quantification of causal relationships between complex ecosystems in response to
352 climate change and enables the analysis of indirect effects among variables.
- 353 2. Compared to BN, the feature importance difference between 'VPD and CSWI' and 'LAI_{max} and Hc'
354 reported by Random forests is higher and can be overestimated.
- 355 3. With the causality relation between correlated variables constructed, BN_{sens} can reduce the uncertainty in
356 quantifying the importance of correlated variables.
- 357 4. The understanding of the mechanism of indirect effects of climate variables on ecosystem function through
358 plant traits can be deepened by the chain causality quantification in BNs.

359

360 **Financial support**

361 This research was supported by the National Natural Science Foundation of China (Grant No. U1803243), the
362 Key projects of the Natural Science Foundation of Xinjiang Autonomous Region (Grant No. 2022D01D01), the
363 Strategic Priority Research Program of the Chinese Academy of Sciences (Grant No. XDA20060302), and
364 High-End Foreign Experts Project.

365 **Author Contributions**

366 HS and GL initiated this research and were responsible for the integrity of the work as a whole. HS performed
367 formal analysis and calculations and drafted the manuscript. HS was responsible for the data collection and
368 analysis. GL, PDM, TVdV, OH, and AK contributed resources and financial support.

369 **Competing interests**

370 The authors declare that they have no conflict of interest.

371 **Code availability**

372 The codes that were used for all analyses are available from the first author (shihaiyang16@mails.ucas.ac.cn)
373 upon request.

374 **Data availability**

375 The data used in this study can be accessed by contacting the first author (shihaiyang16@mails.ucas.ac.cn) upon
376 request.

377

378 **References**

- 379 Anderegg, W. R., Trugman, A. T., Bowling, D. R., Salvucci, G., and Tuttle, S. E.: Plant functional
380 traits and climate influence drought intensification and land–atmosphere feedbacks, *Proceedings of*
381 *the National Academy of Sciences*, 116, 14071–14076, 2019.
- 382 Bairey, E., Kelsic, E. D., and Kishony, R.: High-order species interactions shape ecosystem diversity,
383 *Nat Commun*, 7, 1–7, <https://doi.org/10.1038/ncomms12285>, 2016.
- 384 Baldocchi, D.: Measuring fluxes of trace gases and energy between ecosystems and the atmosphere–
385 the state and future of the eddy covariance method, *Global change biology*, 20, 3600–3609, 2014.
- 386 Barnes, M. L., Farella, M. M., Scott, R. L., Moore, D. J. P., Ponce-Campos, G. E., Biederman, J. A.,
387 MacBean, N., Litvak, M. E., and Breshears, D. D.: Improved dryland carbon flux predictions with
388 explicit consideration of water-carbon coupling, *Commun Earth Environ*, 2, 1–9,
389 <https://doi.org/10.1038/s43247-021-00308-2>, 2021.
- 390 Borchert, R., Calle, Z., Strahler, A. H., Baertschi, A., Magill, R. E., Broadhead, J. S., Kamau, J.,
391 Njoroge, J., and Muthuri, C.: Insolation and photoperiodic control of tree development near the
392 equator, *New Phytologist*, 205, 7–13, 2015.
- 393 Brown, J. H., Gillooly, J. F., Allen, A. P., Savage, V. M., and West, G. B.: Toward a metabolic theory
394 of ecology, *Ecology*, 85, 1771–1789, 2004.
- 395 Chan, T., Ross, H., Hoverman, S., and Powell, B.: Participatory development of a Bayesian network
396 model for catchment-based water resource management, *Water Resour. Res.*, 46,
397 <https://doi.org/10.1029/2009WR008848>, 2010.
- 398 Chapin Iii, F. S., Zavaleta, E. S., Eviner, V. T., Naylor, R. L., Vitousek, P. M., Reynolds, H. L.,
399 Hooper, D. U., Lavorel, S., Sala, O. E., and Hobbie, S. E.: Consequences of changing biodiversity,
400 *Nature*, 405, 234–242, 2000.
- 401 Davidson, E. A. and Janssens, I. A.: Temperature sensitivity of soil carbon decomposition and
402 feedbacks to climate change, *Nature*, 440, 165–173, 2006.
- 403 Diaz, S. and Cabido, M.: Plant functional types and ecosystem function in relation to global change,
404 *Journal of Vegetation Science*, 8, 463–474, <https://doi.org/10.2307/3237198>, 1997.
- 405 Enquist, B. J., Economo, E. P., Huxman, T. E., Allen, A. P., Ignace, D. D., and Gillooly, J. F.: Scaling
406 metabolism from organisms to ecosystems, *Nature*, 423, 639–642, 2003.
- 407 Flanagan, L. B. and Johnson, B. G.: Interacting effects of temperature, soil moisture and plant
408 biomass production on ecosystem respiration in a northern temperate grassland, *Agricultural and*
409 *Forest Meteorology*, 130, 237–253, 2005.
- 410 Flechard, C. R., Ibrom, A., Skiba, U. M., de Vries, W., van Oijen, M., Cameron, D. R., Dise, N. B.,
411 Korhonen, J. F. J., Buchmann, N., Legout, A., Simpson, D., Sanz, M. J., Aubinet, M., Loustau, D.,
412 Montagnani, L., Neiryneck, J., Janssens, I. A., Pihlatie, M., Kiese, R., Siemens, J., Francez, A.-J.,
413 Augustin, J., Varlagin, A., Olejnik, J., Juszczak, R., Aurela, M., Berveiller, D., Chojnicki, B. H.,
414 Dämmgen, U., Delpierre, N., Djuricic, V., Drewer, J., Dufrêne, E., Eugster, W., Fauvel, Y., Fowler,
415 D., Frumau, A., Granier, A., Gross, P., Hamon, Y., Helfter, C., Hensen, A., Horváth, L., Kitzler, B.,
416 Kruijt, B., Kutsch, W. L., Lobo-do-Vale, R., Lohila, A., Longdoz, B., Marek, M. V., Matteucci, G.,
417 Mitasinkova, M., Moreaux, V., Neftel, A., Ourcival, J.-M., Pilegaard, K., Pita, G., Sanz, F.,
418 Schjoerring, J. K., Sebastià, M.-T., Tang, Y. S., Uggerud, H., Urbaniak, M., van Dijk, N., Vesala, T.,
419 Vidic, S., Vincke, C., Weidinger, T., Zechmeister-Boltenstern, S., Butterbach-Bahl, K., Nemitz, E.,

420 and Sutton, M. A.: Carbon–nitrogen interactions in European forests and semi-natural vegetation –
421 Part 1: Fluxes and budgets of carbon, nitrogen and greenhouse gases from ecosystem monitoring and
422 modelling, *Biogeosciences*, 17, 1583–1620, <https://doi.org/10.5194/bg-17-1583-2020>, 2020.

423 Fleischer, K., Wårlind, D., Van der Molen, M. K., Rebel, K. T., Arneth, A., Erisman, J. W., Wassen,
424 M. J., Smith, B., Gough, C. M., and Margolis, H. A.: Low historical nitrogen deposition effect on
425 carbon sequestration in the boreal zone, *Journal of Geophysical Research: Biogeosciences*, 120,
426 2542–2561, 2015.

427 Friedman, N., Geiger, D., and Goldszmidt, M.: Bayesian network classifiers, *Machine learning*, 29,
428 131–163, 1997.

429 Green, J. K., Seneviratne, S. I., Berg, A. M., Findell, K. L., Hagemann, S., Lawrence, D. M., and
430 Gentine, P.: Large influence of soil moisture on long-term terrestrial carbon uptake, *Nature*, 565, 476–
431 479, 2019.

432 Grimm, N. B., Chapin III, F. S., Bierwagen, B., Gonzalez, P., Groffman, P. M., Luo, Y., Melton, F.,
433 Nadelhoffer, K., Pairis, A., and Raymond, P. A.: The impacts of climate change on ecosystem
434 structure and function, *Frontiers in Ecology and the Environment*, 11, 474–482, 2013.

435 de Groot, R. S., Wilson, M. A., and Boumans, R. M. J.: A typology for the classification, description
436 and valuation of ecosystem functions, goods and services, *Ecological Economics*, 41, 393–408,
437 [https://doi.org/10.1016/S0921-8009\(02\)00089-7](https://doi.org/10.1016/S0921-8009(02)00089-7), 2002.

438 Grossiord, C., Buckley, T. N., Cernusak, L. A., Novick, K. A., Poulter, B., Siegwolf, R. T. W.,
439 Sperry, J. S., and McDowell, N. G.: Plant responses to rising vapor pressure deficit, *New Phytologist*,
440 226, 1550–1566, <https://doi.org/10.1111/nph.16485>, 2020.

441 Guisan, A. and Zimmermann, N. E.: Predictive habitat distribution models in ecology, *Ecological*
442 *modelling*, 135, 147–186, 2000.

443 Günter, S., Stimm, B., Cabrera, M., Diaz, M. L., Lojan, M., Ordonez, E., Richter, M., and Weber, M.:
444 Tree phenology in montane forests of southern Ecuador can be explained by precipitation, radiation
445 and photoperiodic control, *Journal of Tropical Ecology*, 24, 247–258, 2008.

446 Humphrey, V., Berg, A., Ciais, P., Gentine, P., Jung, M., Reichstein, M., Seneviratne, S. I., and
447 Frankenberg, C.: Soil moisture–atmosphere feedback dominates land carbon uptake variability,
448 *Nature*, 592, 65–69, <https://doi.org/10.1038/s41586-021-03325-5>, 2021.

449 Jung, M., Reichstein, M., Ciais, P., Seneviratne, S. I., Sheffield, J., Goulden, M. L., Bonan, G.,
450 Cescatti, A., Chen, J., de Jeu, R., Dolman, A. J., Eugster, W., Gerten, D., Gianelle, D., Gobron, N.,
451 Heinke, J., Kimball, J., Law, B. E., Montagnani, L., Mu, Q., Mueller, B., Oleson, K., Papale, D.,
452 Richardson, A. D., Rouspard, O., Running, S., Tomelleri, E., Viovy, N., Weber, U., Williams, C.,
453 Wood, E., Zaehle, S., and Zhang, K.: Recent decline in the global land evapotranspiration trend due to
454 limited moisture supply, *Nature*, 467, 951–954, <https://doi.org/10.1038/nature09396>, 2010.

455 Jung, M., Schwalm, C., Migliavacca, M., Walther, S., Camps-Valls, G., Koirala, S., Anthoni, P.,
456 Besnard, S., Bodesheim, P., Carvalhais, N., Chevallier, F., Gans, F., S Goll, D., Haverd, V., Köhler,
457 P., Ichii, K., K Jain, A., Liu, J., Lombardozzi, D., E M S Nabel, J., A Nelson, J., O’Sullivan, M.,
458 Pallandt, M., Papale, D., Peters, W., Pongratz, J., Rödenbeck, C., Sitch, S., Tramontana, G., Walker,
459 A., Weber, U., and Reichstein, M.: Scaling carbon fluxes from eddy covariance sites to globe:
460 Synthesis and evaluation of the FLUXCOM approach, *Biogeosciences*, 17, 1343–1365,
461 <https://doi.org/10.5194/bg-17-1343-2020>, 2020.

462 Keshtkar, A. R., Salajegheh, A., Sadoddin, A., and Allan, M. G.: Application of Bayesian networks
463 for sustainability assessment in catchment modeling and management (Case study: The Hablehrood
464 river catchment), *Ecological Modelling*, 268, 48–54, 2013.

465 Koch, G. W., Sillett, S. C., Jennings, G. M., and Davis, S. D.: The limits to tree height, *Nature*, 428,
466 851–854, 2004.

467 Konings, A., Williams, A., and Gentine, P.: Sensitivity of grassland productivity to aridity controlled
468 by stomatal and xylem regulation, *Nature Geoscience*, 10, 284–288, 2017.

469 Lansu, E. M., van Heerwaarden, C., Stegehuis, A. I., and Teuling, A. J.: Atmospheric aridity and
470 apparent soil moisture drought in European forest during heat waves, *Geophysical Research Letters*,
471 47, e2020GL087091, 2020.

472 Lin, C., Gentine, P., Frankenberg, C., Zhou, S., Kennedy, D., and Li, X.: Evaluation and mechanism
473 exploration of the diurnal hysteresis of ecosystem fluxes, *Agricultural and Forest Meteorology*, 278,
474 107642, <https://doi.org/10.1016/j.agrformet.2019.107642>, 2019.

475 Liu, L., Gudmundsson, L., Hauser, M., Qin, D., Li, S., and Seneviratne, S. I.: Soil moisture dominates
476 dryness stress on ecosystem production globally, *Nature communications*, 11, 1–9, 2020.

477 Liu, Q., Fu, Y. H., Zeng, Z., Huang, M., Li, X., and Piao, S.: Temperature, precipitation, and
478 insolation effects on autumn vegetation phenology in temperate China, *Global Change Biology*, 22,
479 644–655, <https://doi.org/10.1111/gcb.13081>, 2016.

480 Madani, N., Kimball, J. S., Ballantyne, A. P., Affleck, D. L. R., van Bodegom, P. M., Reich, P. B.,
481 Kattge, J., Sala, A., Nazeri, M., Jones, M. O., Zhao, M., and Running, S. W.: Future global
482 productivity will be affected by plant trait response to climate, *Sci Rep*, 8, 2870,
483 <https://doi.org/10.1038/s41598-018-21172-9>, 2018.

484 Manning, P., Van Der Plas, F., Soliveres, S., Allan, E., Maestre, F. T., Mace, G., Whittingham, M. J.,
485 and Fischer, M.: Redefining ecosystem multifunctionality, *Nature ecology & evolution*, 2, 427–436,
486 2018.

487 Marcot, B. G.: Metrics for evaluating performance and uncertainty of Bayesian network models,
488 *Ecological modelling*, 230, 50–62, 2012.

489 Marcot, B. G. and Hanea, A. M.: What is an optimal value of k in k-fold cross-validation in discrete
490 Bayesian network analysis?, *Comput Stat*, 36, 2009–2031, [https://doi.org/10.1007/s00180-020-00999-](https://doi.org/10.1007/s00180-020-00999-9)
491 9, 2021.

492 Marcot, B. G. and Penman, T. D.: Advances in Bayesian network modelling: Integration of modelling
493 technologies, *Environmental modelling & software*, 111, 386–393, 2019.

494 Migliavacca, M. and Musavi, T.: Reproducible Workflow: The three major axes of terrestrial
495 ecosystem function, <https://doi.org/10.5281/zenodo.5153538>, 2021.

496 Migliavacca, M., Reichstein, M., Richardson, A. D., Colombo, R., Sutton, M. A., Lasslop, G.,
497 Tomelleri, E., Wohlfahrt, G., Carvalhais, N., and Cescatti, A.: Semiempirical modeling of abiotic and
498 biotic factors controlling ecosystem respiration across eddy covariance sites, *Global Change Biology*,
499 17, 390–409, 2011.

500 Migliavacca, M., Musavi, T., Mahecha, M. D., Nelson, J. A., Knauer, J., Baldocchi, D. D., Perez-
501 Priego, O., Christiansen, R., Peters, J., Anderson, K., Bahn, M., Black, T. A., Blanken, P. D., Bonal,
502 D., Buchmann, N., Caldararu, S., Carrara, A., Carvalhais, N., Cescatti, A., Chen, J., Cleverly, J.,

503 Cremonese, E., Desai, A. R., El-Madany, T. S., Farella, M. M., Fernández-Martínez, M., Filippa, G.,
504 Forkel, M., Galvagno, M., Gomasasca, U., Gough, C. M., Göckede, M., Ibrom, A., Ikawa, H.,
505 Janssens, I. A., Jung, M., Kattge, J., Keenan, T. F., Knohl, A., Kobayashi, H., Kraemer, G., Law, B.
506 E., Liddell, M. J., Ma, X., Mammarella, I., Martini, D., Macfarlane, C., Matteucci, G., Montagnani,
507 L., Pabon-Moreno, D. E., Panigada, C., Papale, D., Pendall, E., Penuelas, J., Phillips, R. P., Reich, P.
508 B., Rossini, M., Rotenberg, E., Scott, R. L., Stahl, C., Weber, U., Wohlfahrt, G., Wolf, S., Wright, I.
509 J., Yakir, D., Zaehle, S., and Reichstein, M.: The three major axes of terrestrial ecosystem function,
510 *Nature*, 598, 468–472, <https://doi.org/10.1038/s41586-021-03939-9>, 2021.

511 Milns, I., Beale, C. M., and Smith, V. A.: Revealing ecological networks using Bayesian network
512 inference algorithms, *Ecology*, 91, 1892–1899, <https://doi.org/10.1890/09-0731.1>, 2010.

513 Moles, A. T., Warton, D. I., Warman, L., Swenson, N. G., Laffan, S. W., Zanne, A. E., Pitman, A.,
514 Hemmings, F. A., and Leishman, M. R.: Global patterns in plant height, *Journal of ecology*, 97, 923–
515 932, 2009.

516 Monteith, J. L.: Solar radiation and productivity in tropical ecosystems, *Journal of applied ecology*, 9,
517 747–766, 1972.

518 Moon, T. K.: The expectation-maximization algorithm, *IEEE Signal processing magazine*, 13, 47–60,
519 1996.

520 Musavi, T., Mahecha, M. D., Migliavacca, M., Reichstein, M., van de Weg, M. J., van Bodegom, P.
521 M., Bahn, M., Wirth, C., Reich, P. B., and Schrod, F.: The imprint of plants on ecosystem
522 functioning: A data-driven approach, *International Journal of Applied Earth Observation and*
523 *Geoinformation*, 43, 119–131, 2015.

524 Musavi, T., Migliavacca, M., van de Weg, M. J., Kattge, J., Wohlfahrt, G., van Bodegom, P. M.,
525 Reichstein, M., Bahn, M., Carrara, A., and Domingues, T. F.: Potential and limitations of inferring
526 ecosystem photosynthetic capacity from leaf functional traits, *Ecology and evolution*, 6, 7352–7366,
527 2016.

528 Myers-Smith, I. H., Thomas, H. J. D., and Bjorkman, A. D.: Plant traits inform predictions of tundra
529 responses to global change, *New Phytologist*, 221, 1742–1748, <https://doi.org/10.1111/nph.15592>,
530 2019.

531 Nelson, J. A., Carvalhais, N., Migliavacca, M., Reichstein, M., and Jung, M.: Water-stress-induced
532 breakdown of carbon–water relations: indicators from diurnal FLUXNET patterns, *Biogeosciences*,
533 15, 2433–2447, 2018.

534 Nojavan A., F., Qian, S. S., and Stow, C. A.: Comparative analysis of discretization methods in
535 Bayesian networks, *Environmental Modelling & Software*, 87, 64–71,
536 <https://doi.org/10.1016/j.envsoft.2016.10.007>, 2017.

537 Pastorello, G., Trotta, C., Canfora, E., Chu, H., Christianson, D., Cheah, Y.-W., Poindexter, C., Chen,
538 J., Elbashandy, A., Humphrey, M., Isaac, P., Polidori, D., Reichstein, M., Ribeca, A., van Ingen, C.,
539 Vuichard, N., Zhang, L., Amiro, B., Ammann, C., Arain, M. A., Ardö, J., Arkebauer, T., Arndt, S. K.,
540 Arriga, N., Aubinet, M., Aurela, M., Baldocchi, D., Barr, A., Beamesderfer, E., Marchesini, L. B.,
541 Bergeron, O., Beringer, J., Bernhofer, C., Berveiller, D., Billesbach, D., Black, T. A., Blanken, P. D.,
542 Bohrer, G., Boike, J., Bolstad, P. V., Bonal, D., Bonnefond, J.-M., Bowling, D. R., Bracho, R.,
543 Brodeur, J., Brümmer, C., Buchmann, N., Burban, B., Burns, S. P., Buysse, P., Cale, P., Cavagna, M.,
544 Cellier, P., Chen, S., Chini, I., Christensen, T. R., Cleverly, J., Collalti, A., Consalvo, C., Cook, B. D.,
545 Cook, D., Coursolle, C., Cremonese, E., Curtis, P. S., D’Andrea, E., da Rocha, H., Dai, X., Davis, K.
546 J., Cinti, B. D., Grandcourt, A. de Ligne, A. D., De Oliveira, R. C., Delpierre, N., Desai, A. R., Di
547 Bella, C. M., Tommasi, P. di, Dolman, H., Domingo, F., Dong, G., Dore, S., Duce, P., Dufrêne, E.,

- 548 Dunn, A., Dušek, J., Eamus, D., Eichelmann, U., ElKhidir, H. A. M., Eugster, W., Ewenz, C. M.,
549 Ewers, B., Famulari, D., Fares, S., Feigenwinter, I., Feitz, A., Fensholt, R., Filippa, G., Fischer, M.,
550 Frank, J., Galvagno, M., et al.: The FLUXNET2015 dataset and the ONEFlux processing pipeline for
551 eddy covariance data, *Sci Data*, 7, 225, <https://doi.org/10.1038/s41597-020-0534-3>, 2020.
- 552 Patanè, C.: Leaf Area Index, Leaf Transpiration and Stomatal Conductance as Affected by Soil Water
553 Deficit and VPD in Processing Tomato in Semi Arid Mediterranean Climate, *Journal of Agronomy
554 and Crop Science*, 197, 165–176, <https://doi.org/10.1111/j.1439-037X.2010.00454.x>, 2011.
- 555 Pearl, J.: Bayesian networks: A model of self-activated memory for evidential reasoning, in:
556 Proceedings of the 7th Conference of the Cognitive Science Society, University of California, Irvine,
557 CA, USA, 15–17, 1985.
- 558 Peaucelle, M., Bacour, C., Ciais, P., Vuichard, N., Kuppel, S., Peñuelas, J., Beletti Marchesini, L.,
559 Blanken, P. D., Buchmann, N., and Chen, J.: Covariations between plant functional traits emerge from
560 constraining parameterization of a terrestrial biosphere model, *Global ecology and biogeography*, 28,
561 1351–1365, 2019.
- 562 Piedallu, C. and Gégout, J.-C.: Multiscale computation of solar radiation for predictive vegetation
563 modelling, *Annals of forest science*, 64, 899–909, 2007.
- 564 Pollino, C. A., Woodberry, O., Nicholson, A., Korb, K., and Hart, B. T.: Parameterisation and
565 evaluation of a Bayesian network for use in an ecological risk assessment, *Environmental Modelling
566 & Software*, 22, 1140–1152, <https://doi.org/10.1016/j.envsoft.2006.03.006>, 2007.
- 567 Ramazi, P., Kunegel-Lion, M., Greiner, R., and Lewis, M. A.: Exploiting the full potential of
568 Bayesian networks in predictive ecology, *Methods in Ecology and Evolution*, 12, 135–149,
569 <https://doi.org/10.1111/2041-210X.13509>, 2021.
- 570 Reich, P. B. and Oleksyn, J.: Global patterns of plant leaf N and P in relation to temperature and
571 latitude, *Proceedings of the National Academy of Sciences*, 101, 11001–11006, 2004.
- 572 Reichstein, M., Bahn, M., Mahecha, M. D., Kattge, J., and Baldocchi, D. D.: Linking plant and
573 ecosystem functional biogeography, *Proceedings of the National Academy of Sciences*, 111, 13697–
574 13702, <https://doi.org/10.1073/pnas.1216065111>, 2014.
- 575 Reichstein, M., Camps-Valls, G., Stevens, B., Jung, M., Denzler, J., Carvalhais, N., and Prabhat:
576 Deep learning and process understanding for data-driven Earth system science, *Nature*, 566, 195–204,
577 <https://doi.org/10.1038/s41586-019-0912-1>, 2019.
- 578 Ryan, M. G. and Yoder, B. J.: Hydraulic limits to tree height and tree growth, *Bioscience*, 47, 235–
579 242, 1997.
- 580 Sakschewski, B., von Bloh, W., Boit, A., Poorter, L., Peña-Claros, M., Heinke, J., Joshi, J., and
581 Thonicke, K.: Resilience of Amazon forests emerges from plant trait diversity, *Nature Clim Change*,
582 6, 1032–1036, <https://doi.org/10.1038/nclimate3109>, 2016.
- 583 Santiago, L. S. and Mulkey, S. S.: Leaf productivity along a precipitation gradient in lowland Panama:
584 patterns from leaf to ecosystem, *Trees*, 19, 349–356, <https://doi.org/10.1007/s00468-004-0389-9>,
585 2005.
- 586 Shi, H., Luo, G., Zheng, H., Chen, C., Bai, J., Liu, T., Ochege, F. U., and De Maeyer, P.: Coupling the
587 water-energy-food-ecology nexus into a Bayesian network for water resources analysis and
588 management in the Syr Darya River basin, *Journal of Hydrology*, 581, 124387,
589 <https://doi.org/10.1016/j.jhydrol.2019.124387>, 2020a.

590 Shi, H., Luo, G., Zheng, H., Chen, C., Hellwich, O., Bai, J., Liu, T., Liu, S., Xue, J., Cai, P., He, H.,
591 Ochege, F. U., Van de Voorde, T., and de Maeyer, P.: A novel causal structure-based framework for
592 comparing a basin-wide water–energy–food–ecology nexus applied to the data-limited Amu Darya
593 and Syr Darya river basins, *Hydrology and Earth System Sciences*, 25, 901–925,
594 <https://doi.org/10.5194/hess-25-901-2021>, 2021a.

595 Shi, H., Pan, Q., Luo, G., Hellwich, O., Chen, C., Voorde, T. V. de, Kurban, A., De Maeyer, P., and
596 Wu, S.: Analysis of the Impacts of Environmental Factors on Rat Hole Density in the Northern Slope
597 of the Tianshan Mountains with Satellite Remote Sensing Data, *Remote Sensing*, 13, 4709,
598 <https://doi.org/10.3390/rs13224709>, 2021b.

599 Shi, H., Luo, G., Hellwich, O., Xie, M., Zhang, C., Zhang, Y., Wang, Y., Yuan, X., Ma, X., Zhang,
600 W., Kurban, A., De Maeyer, P., and Van de Voorde, T.: Evaluation of water flux predictive models
601 developed using eddy covariance observations and machine learning: a meta-analysis, *Hydrology and
602 Earth System Sciences Discussions*, 1–21, <https://doi.org/10.5194/hess-2022-90>, 2022a.

603 Shi, H., Luo, G., Hellwich, O., Xie, M., Zhang, C., Zhang, Y., Wang, Y., Yuan, X., Ma, X., Zhang,
604 W., Kurban, A., De Maeyer, P., and Van de Voorde, T.: Variability and uncertainty in flux-site-scale
605 net ecosystem exchange simulations based on machine learning and remote sensing: a systematic
606 evaluation, *Biogeosciences*, 19, 3739–3756, <https://doi.org/10.5194/bg-19-3739-2022>, 2022b.

607 Shi, Y., Jin, N., Ma, X., Wu, B., He, Q., Yue, C., and Yu, Q.: Attribution of climate and human
608 activities to vegetation change in China using machine learning techniques, *Agricultural and Forest
609 Meteorology*, 294, 108146, <https://doi.org/10.1016/j.agrformet.2020.108146>, 2020b.

610 Strobl, C., Boulesteix, A.-L., Kneib, T., Augustin, T., and Zeileis, A.: Conditional variable importance
611 for random forests, *BMC Bioinformatics*, 9, 307, <https://doi.org/10.1186/1471-2105-9-307>, 2008.

612 Toloşi, L. and Lengauer, T.: Classification with correlated features: unreliability of feature ranking
613 and solutions, *Bioinformatics*, 27, 1986–1994, <https://doi.org/10.1093/bioinformatics/btr300>, 2011.

614 Tramontana, G., Jung, M., Schwalm, C. R., Ichii, K., Camps-Valls, G., Ráduly, B., Reichstein, M.,
615 Arain, M. A., Cescatti, A., Kiely, G., Merbold, L., Serrano-Ortiz, P., Sickert, S., Wolf, S., and Papale,
616 D.: Predicting carbon dioxide and energy fluxes across global FLUXNET sites with regression
617 algorithms, *Biogeosciences*, 13, 4291–4313, <https://doi.org/10.5194/bg-13-4291-2016>, 2016.

618 Trifonova, N., Kenny, A., Maxwell, D., Duplisea, D., Fernandes, J., and Tucker, A.: Spatio-temporal
619 Bayesian network models with latent variables for revealing trophic dynamics and functional
620 networks in fisheries ecology, *Ecological Informatics*, 30, 142–158,
621 <https://doi.org/10.1016/j.ecoinf.2015.10.003>, 2015.

622 Wagner, F. H., Hérault, B., Rossi, V., Hilker, T., Maeda, E. E., Sanchez, A., Lyapustin, A. I., Galvão,
623 L. S., Wang, Y., and Aragão, L. E.: Climate drivers of the Amazon forest greening, *PLoS One*, 12,
624 e0180932, 2017.

625 Wang, Z., Zhu, D., Wang, X., Zhang, Y., and Peng, S.: Regressions underestimate the direct effect of
626 soil moisture on land carbon sink variability, *Global Change Biology*,
627 <https://doi.org/10.1111/gcb.16422>, 2022.

628 Weih, M. and Karlsson, P. S.: Growth response of Mountain birch to air and soil temperature: is
629 increasing leaf-nitrogen content an acclimation to lower air temperature?, *New Phytologist*, 150, 147–
630 155, <https://doi.org/10.1046/j.1469-8137.2001.00078.x>, 2001.

631 Wen, X.-F., Yu, G.-R., Sun, X.-M., Li, Q.-K., Liu, Y.-F., Zhang, L.-M., Ren, C.-Y., Fu, Y.-L., and Li,
632 Z.-Q.: Soil moisture effect on the temperature dependence of ecosystem respiration in a subtropical

- 633 Pinus plantation of southeastern China, *Agricultural and Forest Meteorology*, 137, 166–175,
634 <https://doi.org/10.1016/j.agrformet.2006.02.005>, 2006.
- 635 Wever, L. A., Flanagan, L. B., and Carlson, P. J.: Seasonal and interannual variation in
636 evapotranspiration, energy balance and surface conductance in a northern temperate grassland,
637 *Agricultural and Forest Meteorology*, 112, 31–49, [https://doi.org/10.1016/S0168-1923\(02\)00041-2](https://doi.org/10.1016/S0168-1923(02)00041-2),
638 2002.
- 639 Wright, I. J. and Westoby, M.: Leaves at low versus high rainfall: coordination of structure, lifespan
640 and physiology, *New phytologist*, 155, 403–416, 2002.
- 641 Xu, L., Baldocchi, D. D., and Tang, J.: How soil moisture, rain pulses, and growth alter the response
642 of ecosystem respiration to temperature, *Global Biogeochemical Cycles*, 18, 2004.
- 643 Xu, S., McVicar, T. R., Li, L., Yu, Z., Jiang, P., Zhang, Y., Ban, Z., Xing, W., Dong, N., Zhang, H.,
644 and Zhang, M.: Globally assessing the hysteresis between sub-diurnal actual evaporation and vapor
645 pressure deficit at the ecosystem scale: Patterns and mechanisms, *Agricultural and Forest
646 Meteorology*, 323, 109085, <https://doi.org/10.1016/j.agrformet.2022.109085>, 2022.
- 647 Yuan, W., Zheng, Y., Piao, S., Ciais, P., Lombardozzi, D., Wang, Y., Ryu, Y., Chen, G., Dong, W.,
648 Hu, Z., Jain, A. K., Jiang, C., Kato, E., Li, S., Lienert, S., Liu, S., Nabel, J. E. M. S., Qin, Z., Quine,
649 T., Sitch, S., Smith, W. K., Wang, F., Wu, C., Xiao, Z., and Yang, S.: Increased atmospheric vapor
650 pressure deficit reduces global vegetation growth, *Science Advances*, 5, eaax1396,
651 <https://doi.org/10.1126/sciadv.aax1396>, 2019.
- 652 Zhou, S., Yu, B., Huang, Y., and Wang, G.: The effect of vapor pressure deficit on water use
653 efficiency at the subdaily time scale, *Geophysical Research Letters*, 41, 5005–5013,
654 <https://doi.org/10.1002/2014GL060741>, 2014.
- 655 Zhou, S., Williams, A. P., Berg, A. M., Cook, B. I., Zhang, Y., Hagemann, S., Lorenz, R.,
656 Seneviratne, S. I., and Gentile, P.: Land–atmosphere feedbacks exacerbate concurrent soil drought
657 and atmospheric aridity, *Proceedings of the National Academy of Sciences*, 116, 18848–18853, 2019.
- 658